Chapter 12

Advanced MOSFET Models for Circuit Simulators

The modeling of MOS transistors for integrated circuit design has been driven by the needs of digital circuit simulation for many years. The trend toward mixed analog-digital chips creates a necessity for MOSFET models appropriate for analog and RF design [1]. Strong inversion used to be the prevailing MOS operation region, but as a consequence of the technological trend toward shorter channel lengths, off-state leakage constraints, and reduced supply voltages, MOS devices now often operate in the moderate and weak inversion regions [2].

Most of the MOSFET models for computer simulation, from the SPICE Level 1 model to BSIM4, have relied on approximate solutions that are only valid in particular regions of operation connected mathematically to provide continuous solutions. Because the threshold of strong inversion V_T is the key parameter in these regional models, they are also called V_T-based models. The regional approach leads to inaccuracy between regions and consequently this class of models is not accurate enough to represent the moderate inversion region [3], widely employed in low supply voltage circuits.

For the above reasons the industry is turning away from V_T-based MOSFET models. The two main approaches as candidates to replace BSIM3-4 models are inversion-charge based and surface-potential based models. This chapter provides an overview of the approaches taken by the developers of this new generation of models. A summary of the fundamental properties of advanced MOSFET models is presented in [4], a joint paper written by the developers of the main advanced models.

MOSFET MODELING FOR CIRCUIT ANALYSIS AND DESIGN
© World Scientific Publishing Co. Pte. Ltd.
http://www.worldscibooks.com/engineering/6111.html

12.1 Surface potential- vs. inversion charge-based models

In the early 70s, when SPICE MOSFET models began to be developed, the available computing power was very limited. Consequently, simple V_T-based models were adopted in which the surface potential is a very simple function of the input voltage: it is constant for V_{GS} above V_T and it is a linear function of gate voltage below V_T. This results in separate solutions for the different operating regions of the MOSFET, requiring smoothing functions to connect the regions. Despite their limitations, such models have been successfully used for much circuit design work. BSIM4 and MOS Model 9 are modern versions of threshold voltage-based models.

Currently, there are essentially two alternative approaches to V_T-based MOSFET models, namely surface potential-based (ϕ_s-based) [5], [6], [7] and inversion charge-based (Q'_I-based) [8], [9], [10] models. In these two alternative models, the drain current and the terminal charges are indirect functions of the terminal voltages through either the surface potential or the inversion charge density.

Conventional surface potential models based on the original charge-sheet approximation of [11] do not lead to a practical result due to difficulties in introducing velocity saturation effects for short-channels and obtaining closed-form self-consistent charges for the device terminals. Practical ϕ_s-based compact models (MM11 [6], SP [7]) use linearization of the surface potential vs. inversion charge density in a similar way as Q'_I- based models do [4]. With regard to Q'_I-based models, the inversion charge density is approximated using the unified charge control model (UCCM) [9].

Briefly, ϕ_s-based and Q'_I-based models have a common background, but enough differences exist between them to motivate model developers to support one approach rather than the other. In this chapter we will, following the joint paper by model developers [4], briefly review several recent Q'_I -based and ϕ_s-based models.

After selecting an approach to solving the fundamental differential equations, the model developer faces many more challenges due to the non-ideal real devices. These include complex doping profiles and small

MOSFET MODELING FOR CIRCUIT ANALYSIS AND DESIGN
© World Scientific Publishing Co. Pte. Ltd.
http://www.worldscibooks.com/engineering/6111.html

dimensions that lead to a variety of physical effects. Because the complete transistor model, including the different physical effects relevant to advanced technologies, is rather complex, we will limit our presentation to the core models. The reader will find abundant literature concerning most of the models reviewed in this chapter. Here, for the sake of conciseness, we will give only the main references.

12.2 Charge-based models

A practical compact model requires efficient and accurate algorithms to calculate currents, charges and derivatives. Maher and Mead [8] showed that the drain current I_D can be expressed as a very simple function of the area densities of the inversion charge at the source, Q'_{IS}, and the drain, Q'_{ID}. This important result is expressed for a long channel transistor by (3.5.3), repeated below for convenience

$$I_D = \frac{\mu_n W}{L}\left[\frac{Q'^2_{IS} - Q'^2_{ID}}{2nC'_{ox}} - \phi_t\left(Q'_{IS} - Q'_{ID}\right)\right] \tag{12.2.1}$$

where ϕ_t is the thermal voltage and n is the slope factor.

Cunha *et al.* [10] derived expressions, which were shown in Chapter 5, for the total charges and small-signal parameters as a function of the source and drain channel charge densities. Shur's group proposed a single equation for the charge densities as a function of terminal voltages [9], called the Unified Charge Control Model (UCCM). An improved version of UCCM is given by (2.4.58) repeated below

$$V_P - V_C = \phi_t\left[\frac{Q'_{IP} - Q'_I}{nC'_{ox}\phi_t} + \ln\left(\frac{Q'_I}{Q'_{IP}}\right)\right] \tag{12.2.2}$$

where V_C is the channel voltage, V_P is the pinch-off voltage and Q'_{IP} is the value of Q'_I at pinch-off.

Recently, Gummel *et al.* [12] rediscovered basically the same charge equation and proposed a charge-based model called USIM. Q'_I-based models rely on the gradual channel assumption and a linearization of the bulk and inversion charges with respect to the surface potential at a fixed

MOSFET MODELING FOR CIRCUIT ANALYSIS AND DESIGN
© World Scientific Publishing Co. Pte. Ltd.
http://www.worldscibooks.com/engineering/6111.html

gate bias. Because the charge-sheet approximation is not essential in the case of Q'_I-based models, they can accurately represent volume inversion and, as a consequence, they are appropriate to represent multiple gates FETs [13], [14].

12.2.1 *The ACM model*

The initial motivation for the ACM modeling approach came from an analog design in digital CMOS technology carried out in the late 1980's. The use of the MOS gate as a linear capacitor required the calculation of the weak nonlinearities of the MOS capacitor in accumulation and strong inversion. The classical strong inversion (SI) approximation was clearly not appropriate and improved capacitive models of the MOS gate valid for moderate inversion (MI) and accumulation were therefore developed [15].

The use of the new gate capacitor model to achieve a four terminal MOS model accurate in SI and MI, was a natural step forward. The model in [16] used lengthy surface potential-based expressions for current and charges and it was not satisfactory for analog design. The necessity for a symmetrical MOSFET model to describe the series association of transistors became clear at that time [17].

An appropriate MOSFET model was finally achieved in [10]. The symmetry of the transistor with respect to source and drain was obeyed. Rigorous definitions of pinch-off and threshold voltages, essential for consistent and precise models, were given as follows.

The channel charge density for which the diffusion current equals the drift current, designated the pinch-off charge density Q'_{IP}, is given by

$$Q'_{IP} = -nC'_{ox}\phi_t \,. \tag{12.2.3}$$

The channel-to-substrate voltage (V_C) for which the channel charge density equals Q'_{IP} is called the pinch-off voltage V_P.

The accurate expression for the pinch-off voltage is given by (2.4.49), repeated below

$$V_P = \phi_{sa} - 2\phi_F - \phi_t\left(1 + \ln\left(\frac{n}{n-1}\right)\right) \tag{12.2.4}$$

MOSFET MODELING FOR CIRCUIT ANALYSIS AND DESIGN
© World Scientific Publishing Co. Pte. Ltd.
http://www.worldscibooks.com/engineering/6111.html

where ϕ_{sa} is the value of the surface potential deep in weak inversion, neglecting channel charge.

The equilibrium threshold voltage V_{TO}, measured for V_C=0, is the gate voltage for which the channel charge density equals Q'_{IP}.

The linear approximation of V_P can be written as

$$V_P \cong \frac{V_G - V_{T0}}{n}. \tag{12.2.5}$$

Equation (12.2.5) is useful for hand analysis, but the exponential dependence of Q'_I on V_P in weak inversion precludes (12.2.5) or expressions based on approximations of the pinch-off voltage from being used for accurate modeling.

The unified charge control model (UCCM) was derived in [20] adding a new basic approximation to the model in [10]. Considering the inversion capacitance C'_i proportional to the inversion charge it follows that

$$dQ'_I\left(\frac{1}{nC'_{ox}} - \frac{\phi_t}{Q'_I}\right) = dV_C. \tag{12.2.6}$$

Integrating (12.2.6) between an arbitrary channel potential V_C and the pinch-off voltage V_P, yields the UCCM, equation (12.2.2). As shown in Section 2.4.6, the use of the UCCM in conjunction with the pinch-off charge definition, (12.2.3), and the pinch-off voltage expression in (12.2.4) gives a model of the inversion charge essentially equivalent to the conventional surface potential charge-sheet model.

The dc, ac and non-quasi-static models were developed in [18]. The long-channel drain current expression is obtained combining expressions (12.2.1) and (12.2.2). The result was given by equations (3.7.1) and (3.7.7), rewritten below as

$$I_D = I_F - I_R = I(V_G, V_S) - I(V_G, V_D) \tag{12.2.7}$$

$$V_P - V_{S(D)} = \phi_t\left[\sqrt{1 + \frac{I_{F(R)}}{I_S}} - 2 + \ln\left(\sqrt{1 + \frac{I_{F(R)}}{I_S}} - 1\right)\right] \tag{12.2.8}$$

MOSFET MODELING FOR CIRCUIT ANALYSIS AND DESIGN
© World Scientific Publishing Co. Pte. Ltd.
http://www.worldscibooks.com/engineering/6111.html

where I_S is the normalization current given by

$$I_S = \mu_n C'_{ox} n \frac{\phi_t^2}{2} \frac{W}{L}. \tag{12.2.9}$$

Explicit expressions for the current, charges, transconductances and the 16 capacitive coefficients valid in weak, moderate and strong inversion were made available in [18]. All transistor parameters were given as very simple (rational) functions of the inversion charge densities at the channel boundaries.

A computer-implemented version of the model, called ACM (Advanced Compact MOSFET), has been included in a circuit simulator since 1997 [19].

Table 12.1 A complete set of capacitive coefficients for the MOSFET: $q'_{IS(D)} = Q'_{IS(D)}/Q'_{IP}$ and $\alpha = (Q'_{ID} + Q'_{IP})/(Q'_{IS} + Q'_{IP})$

$C_{gs} = \frac{2}{3} C_{ox} \frac{1+2\alpha}{(1+\alpha)^2} \frac{q'_{IS}}{1+q'_{IS}}$
$C_{gd} = \frac{2}{3} C_{ox} \frac{\alpha^2+2\alpha}{(1+\alpha)^2} \frac{q'_{ID}}{1+q'_{ID}}$
$C_{bs(d)} = (n-1) C_{gs(d)}$
$C_{bg} = C_{gb} = \frac{n-1}{n} (C_{ox} - C_{gs} - C_{gd})$
$C_{sd} = -\frac{4}{15} n C_{ox} \frac{\alpha + 3\alpha^2 + \alpha^3}{(1+\alpha)^3} \frac{q'_{ID}}{1+q'_{ID}}$
$C_{ds} = -\frac{4}{15} n C_{ox} \frac{1 + 3\alpha + \alpha^2}{(1+\alpha)^3} \frac{q'_{IS}}{1+q'_{IS}}$
$C_{dg} - C_{gd} = C_m = (C_{sd} - C_{ds})/n$

MOSFET MODELING FOR CIRCUIT ANALYSIS AND DESIGN
© World Scientific Publishing Co. Pte. Ltd.
http://www.worldscibooks.com/engineering/6111.html

ACM has a hierarchical structure that facilitates the inclusion of different phenomena into the model. Because of its very simple expression for the derivative of the channel charge density (12.2.6), ACM was the first, and is still the only model, to furnish simple explicit expressions for all the intrinsic capacitive coefficients (given in Table 5.3 and repeated in Table 12.1).

Parameters of the ACM model can be easily extracted, as shown in [20]. Recently, unified 1/f noise and mismatch models were presented in [21] and [22], respectively.

12.2.2 *The EKV model*

The EKV model was initially developed for the design of very low-power analog ICs, in which transistors operate not only in strong inversion but also in weak and moderate inversion. The EKV model [2] was the first to introduce single-piece analytical expressions for the current, transconductances, intrinsic capacitances, non-quasi-static transadmittances, and noise valid in weak, moderate and strong inversion and from the linear to the saturation region.

The EKV model was obtained from the following approach: the weak and strong inversion asymptotes are first derived; the relevant variables (currents, conductances, etc.) are normalized and finally linked using appropriate interpolation functions. In contrast to most MOSFET models, the EKV model exploited the inherent symmetry of the MOSFET by referring all the terminal voltages to the substrate. As a consequence of the symmetry of the device, the drain current I_D is expressed as the difference between a forward component I_F and a reverse component I_R.

$$I_D = I_F - I_R \,. \tag{12.2.10}$$

Among the important results in [2], the following are worth highlighting.

The normalized forward and reverse currents are defined as $i_f=I_F/I_{spec}$ and $i_r=I_R/I_{spec}$, respectively. I_{spec} is the specific current defined as

$$I_{spec} = 2\mu_n C'_{ox} n \phi_t^2 \frac{W}{L} \,. \tag{12.2.11}$$

MOSFET MODELING FOR CIRCUIT ANALYSIS AND DESIGN
© World Scientific Publishing Co. Pte. Ltd.
http://www.worldscibooks.com/engineering/6111.html

Observe that I_{spec} in EKV is four times larger than I_S in ACM.

The inversion charge density Q_I' is controlled by the voltage difference V_P-V_C, where V_P is the pinch-off voltage and V_C is the channel voltage (difference between the quasi-Fermi potentials of the carriers).

The normalized currents are given in terms of the single variable function G as

$$\frac{I_{F(R)}}{I_{spec}} = i_{f(r)} = G(V_P - V_{S(D)}) . \qquad (12.2.12)$$

EKV evolved into a charge-based formulation when the interpolation function for the continuous g_m/I_D characteristic was substituted by a physics-based expression covering weak to strong inversion [23]. A detailed derivation of the current inversion charge modeling in EKV can be found in [24].

The main equations of ACM and EKV are similar, but there are some differences concerning the pinch-off potential and the slope factor definitions that have some impact on the precision of the inversion charge modeling and consequently deserve some comments. The EKV model uses some empirical parameters to fine tune the inversion charge model that are not necessary in the ACM model.

The pinch-off voltage is defined as the channel voltage for which the inversion charge becomes zero under the strong inversion assumption. The pinch-off voltage in EKV is then computed as[1]

$$V_P = \phi_{sa} - 2\phi_F - m\phi_t \qquad (12.2.13)$$

where m can be considered as a constant, typically ranging between 1 and 4 [24].

In the EKV model, two slope factors are defined, n_q and n_v. n_q is called the inversion charge linearization factor and is given by

$$n_q = 1 + \frac{\gamma}{\sqrt{2\phi_F} + \sqrt{\phi_{sa}}} . \qquad (12.2.14)$$

n_q can be interpreted as a secant between two points on the Q_I' vs. ϕ_s curve. n_v is defined in terms of the derivative of the pinch-off voltage as

[1]In the EKV documentation, ϕ_{sa} is called the pinch-off surface potential (ϕ_P).

MOSFET MODELING FOR CIRCUIT ANALYSIS AND DESIGN
© World Scientific Publishing Co. Pte. Ltd.
http://www.worldscibooks.com/engineering/6111.html

$$n_v = \left[\frac{dV_P}{dV_G}\right]^{-1} = 1 + \frac{\gamma}{2\sqrt{V_P + 2\phi_F + m\phi_t}}. \qquad (12.2.15)$$

Sometimes the nuance between n_q and n_v is disregarded ($n_q \cong n_v \cong n$).

Finally, there is a small difference between ACM and EKV models concerning the value of the inversion charge at pinch-off, *i.e.*, when $V_P - V_{S(D)} = 0$.

The normalization charge is defined in the EKV model as

$$Q'_{spec} = -2n_q C'_{ox}\phi_t. \qquad (12.2.16)$$

The normalized charges $q_{s(d)} = Q'_{IS(D)} / Q'_{spec}$ are dependent on the normalized terminal voltages according to [24]

$$v_p - v_{s(d)} = 2q_{s(d)} + \ln q_{s(d)}, \qquad (12.2.17)$$

where the voltages are normalized with respect to the thermal voltage. The inversion charge for $v_p - v_{s(d)} = 0$ is

$$Q'_I(v_p = v_{s(d)}) = 0.852(-n_q C'_{ox}\phi_t) \qquad (12.2.18)$$

while in ACM the inversion charge at pinch-off is equal to the normalization charge $-nC'_{ox}\phi_t$.

The EKV charge-based model has now evolved into a full-featured compact model that includes all the major effects that have to be accounted for in deep submicron CMOS technologies (for details, visit http://legwww.epfl.ch/ekv).

12.2.3 *The BSIM5 model*

The BSIM5 model was introduced in [25]. It uses the standard charge-based expression for the current given by Eq. (12.2.1). The inversion charge density is calculated through the UCCM using a linearized expression of the pinch-off voltage in terms of the gate voltage. In the literature available on BSIM5 there is some ambiguity concerning the exact expression used for the slope factor n. Poly-depletion and quantum effects are handled by using correction terms for the slope factor and the effective bulk potential. Velocity saturation, velocity overshoot and

MOSFET MODELING FOR CIRCUIT ANALYSIS AND DESIGN
© World Scientific Publishing Co. Pte. Ltd.
http://www.worldscibooks.com/engineering/6111.html

source-velocity limits are modeled in a unified way. An interesting feature of BSIM5 [26] is the use of a simple empirical expression for the bulk charge valid from accumulation to strong inversion (see problem 12.1).

12.3 Surface potential models

The development of ϕ_s-based models for circuit simulation began soon after the development of the charge-sheet theory in 1978-79. In [27] short- and narrow-channel effects were included in the surface potential model of the drain current. Other surface potential models were developed [28], [29], but until recently ϕ_s-based models were considered too complicated for compact modeling.

Applying the gradual channel and charge-sheet assumptions yields the implicit relation for the surface potential presented in Section 2.4.2 and repeated below for convenience

$$\left(V_G - V_{FB} - \phi_s\right)^2 = \gamma^2 \phi_t [e^{-\phi_s/\phi_t} + \phi_s/\phi_t - 1 + e^{-(2\phi_F + V_C)/\phi_t}\left(e^{\phi_s/\phi_t} - \phi_s/\phi_t - 1\right)]. \tag{12.3.1}$$

The accurate solution of (12.3.1), once a big issue, is no longer a problem; in fact, the surface potential can be calculated within machine tolerances and with no significant burden in relation to the overall compact model calculations [30].

After determining the surface potential, the charge-sheet approximation allows a straightforward calculation of the charge densities. The charge-sheet approximation neglects the potential drop across the inversion layer for the calculation of the bulk charge density Q'_B. According to the charge-sheet approximation, Q'_B is given by

$$Q'_B = -sign(\phi_s) C'_{ox} \gamma \sqrt{\phi_s + \phi_t\left(e^{-\phi_s/\phi_t} - 1\right)}. \tag{12.3.2}$$

Expression (12.3.2) gives a continuous model from accumulation through depletion to inversion, unlike the simplified form (12.3.3), which is invalid in accumulation. The even simpler form (12.3.4), often

MOSFET MODELING FOR CIRCUIT ANALYSIS AND DESIGN
© World Scientific Publishing Co. Pte. Ltd.
http://www.worldscibooks.com/engineering/6111.html

employed for calculations of Q_I', is invalid even in weak accumulation as can be seen in Fig. 12.1.

$$Q_{B1}' = -C_{ox}'\gamma\sqrt{\phi_s - \phi_t} \tag{12.3.3}$$

$$Q_{B2}' = -C_{ox}'\gamma\sqrt{\phi_s}\ . \tag{12.3.4}$$

The inversion charge density Q_I' is given by (2.4.33), repeated below

$$Q_I' = -C_{ox}'\left(V_G - V_{FB} - \phi_s + \frac{Q_B'}{C_{ox}'}\right). \tag{12.3.5}$$

Finally, the gate electrode charge per unit area is given by

$$Q_G' = -Q_B' - Q_I' = C_{ox}'\left(V_G - V_{FB} - \phi_s\right). \tag{12.3.6}$$

Summarizing, for ϕ_s-based models, one can calculate ϕ_s iteratively using (12.3.1) and the resultant value is used to calculate Q_B', Q_I' and, Q_G' from (12.3.2), (12.3.5) and (12.3.6), respectively.

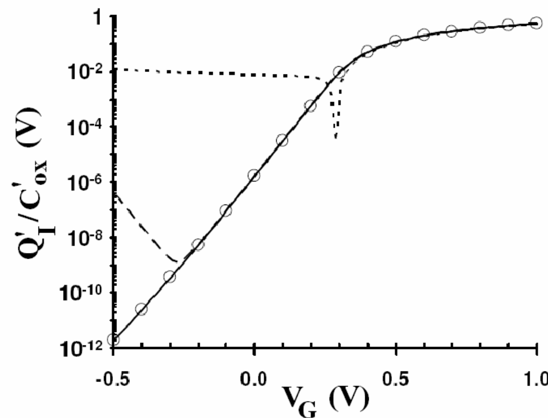

Fig. 12.1 Inversion charge density calculated with (12.3.2), full line, (12.3.3), dashed line, and (12.3.4), dotted line. Circles are results from full numerical solutions of the Poisson equation. (After [4].)

MOSFET MODELING FOR CIRCUIT ANALYSIS AND DESIGN
© World Scientific Publishing Co. Pte. Ltd.
http://www.worldscibooks.com/engineering/6111.html

12.3.1 *The HiSIM model*

HiSIM (Hiroshima-University STARC IGFET Model) calculates the potentials by solving the Poisson equation iteratively at both the source and drain sides. An accuracy of 10 pV has been achieved with faster simulation times than some threshold voltage-based models [5]. Such an extreme accuracy in the surface potential calculations has turned out to be absolutely necessary for maintaining sufficiently accurate solutions for transcapacitance values as well as for achieving stable circuit simulations.

HiSIM is based on the charge-sheet approximation, as are other surface potential models, but avoids the inversion charge (Q'_I) vs. surface potential linearization (ϕ_s) employed in MM11 and SP models. The basic drain current law (for constant mobility) in HiSIM is given by equations (3.4.8), (3.4.9) and (3.4.10), repeated below for convenience

$$I_D = I_{drift} + I_{diff} \tag{12.3.7}$$

$$\begin{aligned} I_{drift} = \mu_n \frac{W}{L} C'_{ox} \Big\{ & (V_G - V_{FB})(\phi_{sL} - \phi_{s0}) - \frac{1}{2}(\phi_{sL}^2 - \phi_{s0}^2) \\ & - \frac{2}{3}\gamma[(\phi_{sL} - \phi_t)^{3/2} - (\phi_{s0} - \phi_t)^{3/2}] \Big\} \end{aligned} \tag{12.3.8}$$

$$\begin{aligned} I_{diff} = \mu_n \frac{W}{L} C'_{ox} \phi_t \{ & (\phi_{sL} - \phi_{s0}) \\ & + \gamma[(\phi_{sL} - \phi_t)^{1/2} - (\phi_{s0} - \phi_t)^{1/2}] \}. \end{aligned} \tag{12.3.9}$$

Without linearization of Q'_I vs. ϕ_s, the model equations, particularly those for the intrinsic charges, are complicated. As an example, the total depletion charge for $V_{BS}=0$ is given by

MOSFET MODELING FOR CIRCUIT ANALYSIS AND DESIGN
© World Scientific Publishing Co. Pte. Ltd.
http://www.worldscibooks.com/engineering/6111.html

$$Q_B = -\frac{\mu_n W^2}{I_D}\left\{ C'_{ox} q N_{sub} L_D \frac{2\sqrt{2}}{3\beta}\left(V'_G - \phi_s\right)\left(\beta\phi_s - 1\right)^{3/2}\Big|_{\phi_{s0}}^{\phi_{sL}} \right.$$
$$+ C'_{ox} q N_{sub} L_D \frac{2\sqrt{2}}{3\beta^2}\left[\frac{2}{5}\left(\beta\phi_s - 1\right)^{5/2} + \left(\beta\phi_s - 1\right)^{3/2}\right]\Big|_{\phi_{s0}}^{\phi_{sL}} \qquad (12.3.10)$$
$$\left. + \left(q N_{sub} L_D \sqrt{2}\right)^2 \left[\frac{\phi_s}{2}\left(3 - \beta\phi_s\right)\right]\Big|_{\phi_{s0}}^{\phi_{sL}} \right\}$$

where N_{sub} is the substrate doping, L_D is the extrinsic Debye length, β is the reciprocal of the thermal voltage, the other symbols have their usual meaning, and V'_G, given below, is a shifted gate voltage that accounts for short-channel effects.

In a surface potential model, short-channel effects can no longer be accounted for by simply adding new terms to the expression for the threshold voltage. This problem has been gradually solved in the modern ϕ_s-based models by accumulating the necessary experience and trying different approaches. In both HiSIM and SP models, the bias and geometry-dependent lateral-gradient factor originally introduced in [31] [31] are employed. In this approach [5], the gate-to-source voltage V_{gs} is shifted by a value that depends on the lateral electrical field F_{yy} as shown below

$$V'_G = V_{gs} + \Delta V'_G - V_{FB}$$
$$\Delta V'_G = \frac{\varepsilon_s}{C'_{ox}}\sqrt{\frac{2\varepsilon_s}{qN_{sub}}\left[\phi_s(y) - V_{bs} - \phi_t\right]} F_{yy} \qquad (12.3.11)$$
$$F_{yy} = \frac{dF_y}{dy}.$$

The gradient of the lateral electrical field F_{yy} is assumed to be independent of position owing to a parabolic approximation of the electrostatic potential along the channel. F_{yy} is extracted from measured threshold voltage vs. bias characteristics.

MOSFET MODELING FOR CIRCUIT ANALYSIS AND DESIGN
© World Scientific Publishing Co. Pte. Ltd.
http://www.worldscibooks.com/engineering/6111.html

12.3.2 *MOS model 11*

MOS Model 11 (MM11) [6] is the successor to MOS Model 9 [32]. Its development, started in 1994, is aimed at fulfilling the requirements for a model that satisfies the accuracy demands of analog and RF circuit design but with a computational complexity which allows its application in digital designs.

To obtain efficient expressions for model outputs, several approximations were developed mainly based on a linearization of the inversion charge as a function of ϕ_s. In MM11, a linearization is performed around the average of the source and drain surface potentials [6], which results in simpler expressions without loss of accuracy.

The basic drain current expression in MM11 is the same as that given in equation (3.4.16), repeated below for convenience

$$I_D = -\frac{W}{L}\mu_n(\overline{Q}_I' - n_e C_{ox}'\phi_t)(\phi_{sL} - \phi_{s0}). \qquad (12.3.12)$$

In the MM11 documentation, (12.3.12) is written as[2]

$$I_D = -\beta \frac{\overline{Q}*_{inv}}{C_{ox}'}\Delta\psi \qquad (12.3.13)$$

where $\beta = \mu_n C_{ox}' \frac{W}{L}$, $\overline{Q}*_{inv} = \overline{Q_I'} - n_e C_{ox}'\phi_t$, $\Delta\psi = (\phi_{sL} - \phi_{s0})$ and C_{ox}' is the gate oxide capacitance per unit area. $\overline{Q}_I'$, the "average" charge density and the effective capacitance $n_e C_{ox}'$ are calculated at the average surface potential $(\phi_{sL} + \phi_{s0})/2$.

In addition, the MM11 approach also ensures that the model symmetry with respect to source-drain interchange is maintained. Note that this approach is not unlike the symmetric linearization method used in SP [7], which made it easy to merge MM11 and SP into one model called PSP.

For the description of realistic devices, however, the model has to be extended with an accurate description of mobility effects and conductance effects. In MM11, these effects have been added with a particular emphasis on distortion modeling.

---

[2]In the MM11 manual, C_{ox}' is written as C_{ox}

MOSFET MODELING FOR CIRCUIT ANALYSIS AND DESIGN
© World Scientific Publishing Co. Pte. Ltd.
http://www.worldscibooks.com/engineering/6111.html

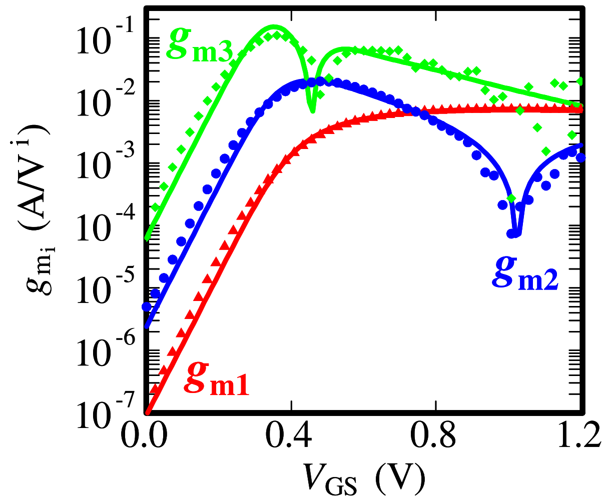

Fig. 12.2 MM11 gives an accurate description of distortion behavior. Measured (symbols) and modeled (lines) higher-order derivatives g_{mi} ($=\partial^i I_D/\partial V_{GS}{}^i$) as a function of gate bias V_{GS} for W/L=10µm/0.1µm device (n-MOS, V_{DS}=0.73V, V_{SB}=0V). (After [4].)

For an accurate description of distortion, the model should accurately describe the drain current and its higher-order derivatives (up to at least 3rd-order). MM11 was specially developed for this purpose. MM11 contains improved expressions for mobility reduction, velocity saturation and various conductance effects [6]. The distortion modeling of MM11 has been extensively tested on various MOSFET technologies, and it gives an accurate description of modern CMOS technologies, as seen in Fig. 12.2.

For modern CMOS technologies several physical effects that did not affect circuit design in the past have become important. All these effects should be described by the compact MOS model. MM11 includes an accurate description of all important physical effects, such as poly-depletion, quantum-mechanical effects, the effect of pocket implants, gate tunneling current, and gate-induced drain leakage [6].

The total source and drain charges for the dynamic modeling of the transistor in MM11 are given by expressions equivalent to (5.2.20) and (5.2.21), repeated below

MOSFET MODELING FOR CIRCUIT ANALYSIS AND DESIGN
© World Scientific Publishing Co. Pte. Ltd.
http://www.worldscibooks.com/engineering/6111.html

$$Q_D = WL\left[\frac{6Q_R'^3 + 12Q_F'Q_R'^2 + 8Q_F'^2Q_R' + 4Q_F'^3}{15\left(Q_F' + Q_R'\right)^2} + \frac{n}{2}C_{ox}'\phi_t\right] \quad (12.3.14)$$

$$Q_S = WL\left[\frac{6Q_F'^3 + 12Q_R'Q_F'^2 + 8Q_R'^2Q_F' + 4Q_R'^3}{15\left(Q_F' + Q_R'\right)^2} + \frac{n}{2}C_{ox}'\phi_t\right]. \quad (12.3.15)$$

Rewriting (12.3.14) and (12.3.15) changing the notation as indicated below

$$\begin{aligned} &-nC_{ox}' \rightarrow C_{inv} \\ &Q_{F(R)}' = Q_{IS(D)}' - nC_{ox}'\phi_t \rightarrow Q_{inv0(L)} + \phi_t C_{inv} = Q_{inv0(L)}^{*} \end{aligned} \quad (12.3.16)$$

the charge expressions as written in MM11 documentation are obtained. Clearly, the total charge expressions used in MM11 use the inversion charge density as the key variable and not the surface potential. If, concerning the input equation, MM11 is surface potential-based, concerning the output equations it is a mixed model. The current is given by (12.3.13) which combines surface potential and charge while the total charges (12.3.14) and (12.3.15), and even the 1/f noise expression, are given in terms of the inversion charge densities at the channel ends.

12.3.3 *The SP model*

The main characteristics of the SP model can be summarized as follows [7]: ϕ_s-based, substrate-referenced with analytic (non-iterative) computation of ϕ_s from accumulation to inversion, symmetric with respect to source-drain interchange, and physics-based modeling of small-geometry effects via lateral field gradient, as in HiSIM.

The search for an approximate analytical solution of the surface potential master equation was initiated in [28] using smoothing functions to connect the asymptotic solutions in subthreshold and strong inversion. However, even the best approximations of this type [33] have an accuracy of 2–3 mV which is not sufficient for the modeling of transconductances and transcapacitances. By using a different approach, SP obtains an approximate solution of (12.3.1) with accuracy better than

MOSFET MODELING FOR CIRCUIT ANALYSIS AND DESIGN
© World Scientific Publishing Co. Pte. Ltd.
http://www.worldscibooks.com/engineering/6111.html

1 nV [34]. As shown in Fig. 12.3, the accuracy of the SP algorithm is the same as that in [34], but now the accumulation region is included.

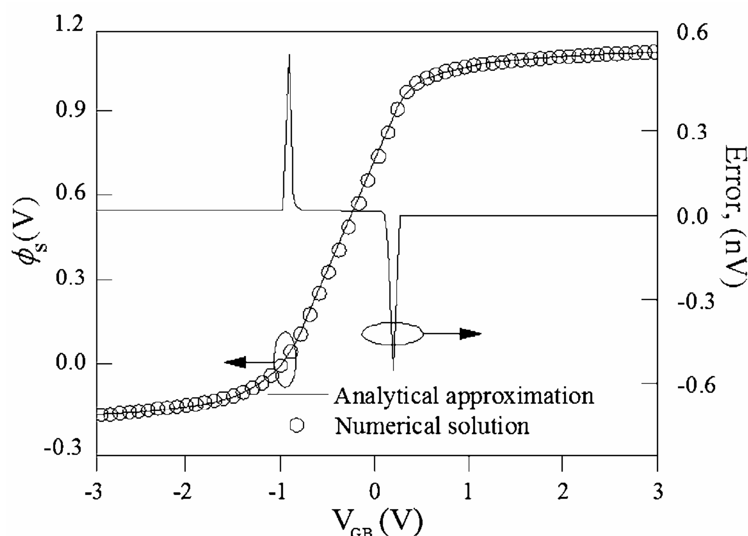

Fig.12.3 Comparison of the analytical approximation of the surface potential in the channel area with numerical solution: N_{sub}=5x10^{17} cm^{-3}, t_{ox}= 25 Å, V_{FB}= -1 V, T=300 K. (After [7].)

Bibliography

[1] Yannis Tsividis and Guido Masetti, "Problems in precision modeling of the MOS transistor for analog applications," *IEEE Trans. Computer-Aided Design*, vol. 3, no. 1, pp. 72-79, Jan. 1984.

[2] Christian C. Enz, François Krummenacher and Eric A. Vittoz, "An analytical MOS transistor model valid in all regions of operation and dedicated to low-voltage and low-current applications," *J. Analog Integr. Circuits Signal Process.,* vol. 8, pp. 83-114, July 1995.

[3] Y. Tsividis, "Moderate inversion in MOS devices," *Solid-State Electron*, vol. 25, no. 11, pp. 1099-1104, Nov. 1982. See also Erratum, ibid, vol. 26, no. 8, p. 823, Aug. 1983.

[4] Josef Watts, Colin McAndrew, Christian Enz, Carlos Galup-Montoro, Gennady Gildenblat, Chenming Hu, Ronald van Langevelde, Mitiko Miura-Mattausch, Rafael Rios, Chih-Tang Sah, "Advanced compact models for MOSFETs," *Proc. Workshop on Compact Modeling*, *Nanotech 2005*, pp. 3-12.

[5] Mitiko Miura-Mattausch, Uwe Feldmann, Alexander Rahm, Michael Bollu, and Dominique Savignac, "Unified complete MOSFET model for analysis of digital

MOSFET MODELING FOR CIRCUIT ANALYSIS AND DESIGN
© World Scientific Publishing Co. Pte. Ltd.
http://www.worldscibooks.com/engineering/6111.html

and analog circuits," *IEEE Trans. Computer-Aided Design*, vol. 15, no. 1, pp. 1–7, Jan. 1996.

[6] R. van Langevelde, A. J. Scholten, and D. B. M. Klaassen, "Physical background of MOS Model 11," Nat. Lab. Unclassified Report 2003/00239. [On line] Available: http://www.semiconductors.philips.com/Philips_Models/

[7] Gennady Gildenblat, Hailing Wang, Ten-Lon Chen, Xin Gu, and Xiaowen Cai, "SP: An advanced surface-potential-based compact MOSFET model," *IEEE J. Solid-State Circuits*, vol. 39, no. 9, pp. 1394-1406, Sep. 2004.

[8] Mary Ann Maher and Carver A. Mead, "A physical charge-controlled model for MOS transistors," in *Advanced Research in VLSI*, P. Losleben (ed.), MIT Press, Cambridge, MA, pp. 211-229, 1987.

[9] Young Hee Byun, Kwyro Lee, and Michael Shur, "Unified charge control model and subthreshold current in heterostructure field effect transistors," *IEEE Electron Device Lett.*, vol. 11, no. 1, pp. 50-53, Jan. 1990.

[10] Ana Isabela Araújo Cunha, Márcio Cherem Schneider, and Carlos Galup-Montoro, "An explicit physical model for the long-channel MOS transistor including small-signal parameters," *Solid-State Electron.,* vol. 38, no. 11, pp. 1945-1952, Nov. 1995.

[11] J. R. Brews, "A charge-sheet model of the MOSFET," *Solid-State Electron.*, vol. 21, no. 2, pp. 345-355, Feb. 1978.

[12] Hermann K. Gummel and Kumud Singhal, "Inversion charge modeling," *IEEE Trans. Electron Devices*, vol. 48, no. 8, pp. 1585-1593, Aug. 2001.

[13] Benjamin Iñíguez, David Jiménez, Jaume Roig, Hamdy A. Hamid, Lluís F. Marsal, and Josep Pallarès, "Explicit continuous model for long-channel undoped surrounding gate MOSFETs," *IEEE Trans. Electron Devices*, vol. 52, no. 8, pp. 1868-1873, Aug. 2005.

[14] Giorgio Mugnaini and Giuseppe Iannaccone, "Physics-based compact model of nanoscale MOSFETs-Part I: transition from drift-diffusion to ballistic transport", *IEEE Trans. Electron Devices*, vol. 52, no. 8, pp. 1795-1801, Aug. 2005.

[15] Alexandre Ternes Behr, Márcio Cherem Schneider, Sidnei Noceti Filho, and Carlos Galup Montoro, "Harmonic distortion caused by capacitors implemented with MOSFET gates," *IEEE J. Solid-State Circuits*, vol. 27, no. 10, pp. 1470-1475, Oct. 1992.

[16] A. I. A. Cunha, R. T. Gonçalves, M. C. Schneider, and C. G. Montoro, "An accurate and explicit physical model of the MOS transistor", *Proc. of the 8th Brazilian Conference on Microelectronics*, 1993, Campinas, Brazil, pp. V7-V12.

[17] Carlos Galup-Montoro, Márcio C. Schneider, and Itamar J. B. Loss, "Series-parallel association of FET's for high gain and high frequency applications," *IEEE J. Solid-State Circuits*, vol. 29, no. 9, pp. 1094-1101, Sep. 1994.

[18] Ana Isabela Araújo Cunha, Márcio Cherem Schneider, and Carlos Galup-Montoro, "An MOS transistor model for analog circuit design," *IEEE J. Solid-State Circuits*, vol. 33, no. 10, pp. 1510-1519, Oct. 1998.

[19] Application Notes in Home-page Dolphin. [Online]. Available: http://www.dolphin.fr/medal/smash/notes/acm_report.pdf

MOSFET MODELING FOR CIRCUIT ANALYSIS AND DESIGN
© World Scientific Publishing Co. Pte. Ltd.
http://www.worldscibooks.com/engineering/6111.html

[20] Ana Isabela Araújo Cunha, Márcio Cherem Schneider, and Carlos Galup-Montoro, "Derivation of the unified charge control model and parameter extraction procedure," *Solid-State Electron.*, vol. 43, no. 3, pp. 481-485, Mar. 1999.

[21] Alfredo Arnaud and Carlos Galup-Montoro, "A compact model for flicker noise in MOS transistors for analog circuit design," *IEEE Trans. Electron Devices*, vol. 50, no. 8, pp. 1815-1818, Aug. 2003.

[22] Carlos Galup-Montoro, Márcio C. Schneider, Hamilton Klimach, and Alfredo Arnaud, "A compact model of MOSFET mismatch for circuit design," *IEEE J. Solid-State Circuits*, vol. 40, no. 8, pp. 1649-1657, Aug. 2005.

[23] Matthias Bucher, *Analytical MOS Transistor Modelling for Analog Circuit Simulation*, PhD Thesis, EPFL, Lausanne, Switzerland, 1999.

[24] Jean-Michel Sallese, Matthias Bucher, François Krummenacher, and Pierre Fazan, "Inversion charge linearization in MOSFET modeling and rigorous derivation of the EKV compact model," *Solid-State Electron.* vol. 47, no. 4, pp. 677–683, Apr. 2003.

[25] Jin He, Xuemei Xi, Mansun Chan, Ali Niknejad, and Chenming Hu, "An advanced surface potential-plus MOSFET model," *Proc. Workshop on Compact Modeling*, *Nanotech 2003*, pp. 262-265.

[26] Ali Niknejad, BSIM5 presentation. [Online]. Available: http://www.eigroup.org/ cmc/next_gen_cmos/bsim5latest.pdf

[27] P. P. Guebels and F. Van de Wiele, "A charge sheet model for small geometry MOSFET's," *IEDM Tech. Dig., 1981*, pp. 211-214.

[28] ClaudioTurchetti and Guido Masetti, "A CAD-oriented analytical MOSFET model for high-accuracy applications," *IEEE Trans. Computer-Aided Design*, vol. 3, no. 2, pp. 117-122, Apr. 1984.

[29] A. R. Boothroyd, Stan W. Tarasewicz, and Cezary Slaby, "MISNAN - A physically based continuous MOSFET model for CAD applications," *IEEE Trans. Computer-Aided Design*, vol. 10, no. 12, pp. 1512-1529, Dec. 1991.

[30] Rafael Rios, Sivakumar Mudanai, Wei-Kai Shih, and Paul Packan, "An efficient surface potential solution algorithm for compact MOSFET models," *IEDM Tech. Dig*., 2004, pp. 755-758.

[31] Mitiko Miura-Mattausch and Hermann Jacobs, "Analytical model for circuit simulation with quarter micron metal oxide semiconductor field effect transistors: subthreshold characteristics," *Jap. J. App. Phys.*, vol. 29, no. 12, pp. 2279-2282, Dec. 1990.

[32] R. M. D. A. Velghe, D. B. M. Klaassen, F. M. Klaassen, "MOS Model 9," NL-UR 003/94, Philips Electronics N.V. [Online]. Available: http://www.semiconductors.philips.com/ Philips_Models/

[33] Ronald van Langevelde and François M. Klaassen, "An explicit surface-potential-based MOSFET model for circuit simulation," *Solid-State Electron.*, vol. 44, no. 3, pp. 409-418, Mar. 2000.

[34] T.-L. Chen and G. Gildenblat, "Analytical approximation for the MOSFET surface potential," *Solid-State Electron.*, vol. 45, no. 2, pp. 335-339, Feb. 2001.

MOSFET MODELING FOR CIRCUIT ANALYSIS AND DESIGN
© World Scientific Publishing Co. Pte. Ltd.
http://www.worldscibooks.com/engineering/6111.html

Problems

12.1. (a) Verify that, in inversion, the bulk charge density can be written as

$$Q'_B \cong -\gamma C'_{ox}\sqrt{\phi_s} \cong -\gamma C'_{ox}\left(\sqrt{V_G - V_{FB} + \frac{Q'_I}{C'_{ox}} + \frac{\gamma^2}{4}} - \frac{\gamma}{2}\right).$$

(b) What is the asymptotic value of the bulk charge deep in accumulation?

(c) Combine the results of items (a) and (b) to demonstrate that the smoothing function

$$Q'_B \cong -C'_{ox}\frac{V_G - V_{FB} + \frac{Q'_I}{C'_{ox}}}{\frac{1}{2} + \sqrt{\frac{V_G - V_{FB} + \frac{Q'_I}{C'_{ox}}}{2\gamma^2} + \frac{1}{4} + \frac{1}{2}\left[\sqrt{\left(\frac{V_G - V_{FB} + \frac{Q'_I}{C'_{ox}}}{\gamma^2}\right)^2 + \delta}\right]}}$$

with δ<<1 represents correctly the asymptotic behavior of the bulk charge. This result for the bulk charge was previously presented on page 19 of reference [26].

MOSFET MODELING FOR CIRCUIT ANALYSIS AND DESIGN
© World Scientific Publishing Co. Pte. Ltd.
http://www.worldscibooks.com/engineering/6111.html